AD-A188416

US Army Corps of Engineers

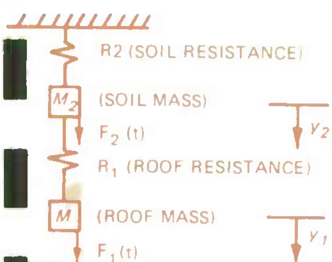

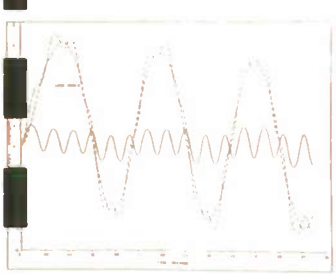

STRUCTURES LABORATORY

TECHNICAL REPORT SL-87-27

IMPORTANCE OF RIGID-BODY MOTIONS ON A SINGLE-DEGREE-OF-FREEDOM MODEL

by

Robert L. Hall

Structures Laboratory

DEPARTMENT OF THE ARMY
Waterways Experiment Station, Corps of Engineers
PO Box 631, Vicksburg, Mississippi 39180-0631

US ARMY ENGINEER WATERWAYS EXPERIMENT STATION

September 1987

Final Report

Approved For Public Release, Distribution Unlimited

Prepared for Defense Nuclear Agency
Washington, DC 20305

Unclassified

SECURITY CLASSIFICATION OF THIS PAGE

REPORT DOCUMENTATION PAGE

1a. REPORT SECURITY CLASSIFICATION Unclassified	1b. RESTRICTIVE MARKINGS
2a. SECURITY CLASSIFICATION AUTHORITY 2b. DECLASSIFICATION / DOWNGRADING SCHEDULE	3. DISTRIBUTION / AVAILABILITY OF REPORT Approved for public release; distribution unlimited.
4. PERFORMING ORGANIZATION REPORT NUMBER(S) Technical Report SL-87-27	5. MONITORING ORGANIZATION REPORT NUMBER(S)
6a. NAME OF PERFORMING ORGANIZATION USAEWES Structures Laboratory — 6b. OFFICE SYMBOL (If applicable) WESSS	7a. NAME OF MONITORING ORGANIZATION
6c. ADDRESS (City, State, and ZIP Code) PO Box 631 Vicksburg, MS 39180-0631	7b. ADDRESS (City, State, and ZIP Code)
8a. NAME OF FUNDING/SPONSORING ORGANIZATION Defense Nuclear Agency — 8b. OFFICE SYMBOL (If applicable)	9. PROCUREMENT INSTRUMENT IDENTIFICATION NUMBER
8c. ADDRESS (City, State, and ZIP Code) Washington, DC 20305	10. SOURCE OF FUNDING NUMBERS PROGRAM ELEMENT NO. / PROJECT NO. / TASK NO. / WORK UNIT ACCESSION NO.

11. TITLE (Include Security Classification)

Importance of Rigid-Body Motions on a Single-Degree-of-Freedom Model

12. PERSONAL AUTHOR(S)
Hall, Robert L.

13a. TYPE OF REPORT	13b. TIME COVERED	14. DATE OF REPORT (Year, Month, Day)	15. PAGE COUNT
Final report	FROM ____ TO ____	September 1987	27

16. SUPPLEMENTARY NOTATION
Available from National Technical Information Service, 5285 Port Royal Road, Springfield, VA 22161

17. COSATI CODES			18. SUBJECT TERMS (Continue on reverse if necessary and identify by block number)
FIELD	GROUP	SUB-GROUP	Rigid-body motion Soil-structure interaction

19. ABSTRACT (Continue on reverse if necessary and identify by block number)

The study presents the effect of rigid-body motion on the single-degree-of-freedom (SDOF) model presently used for dynamic analyses of buried roof slabs. The effect of rigid-body motion is incorporated by adding a second degree of freedom to the model. Relative displacements between the roof and the structure are given for comparison.

The results indicate that at overpressures required to cause severe damage to a relatively hard, shallow-buried structure, rigid-body motion will have little effect on the damage predicted from an SDOF analysis.

20. DISTRIBUTION / AVAILABILITY OF ABSTRACT ☒ UNCLASSIFIED/UNLIMITED ☐ SAME AS RPT. ☐ DTIC USERS	21. ABSTRACT SECURITY CLASSIFICATION Unclassified
22a. NAME OF RESPONSIBLE INDIVIDUAL	22b. TELEPHONE (Include Area Code) — 22c. OFFICE SYMBOL

DD FORM 1473, 84 MAR — 83 APR edition may be used until exhausted. All other editions are obsolete.

SECURITY CLASSIFICATION OF THIS PAGE

Unclassified

Preface

This study was conducted during the period December 1986 through May 1987 by the US Army Engineer Waterways Experiment Station (WES) under the sponsorship of the Defense Nuclear Agency (DNA). Mr. Jim Cooper was the DNA Project Monitor.

The investigation was conducted under the general supervision of Messrs. Bryant Mather, Chief, Structures Laboratory (SL), and James T. Ballard, Assistant Chief, SL, and under the direct supervison of Dr. Jimmy P. Balsara, Chief, Structural Mechanics Division (SMD), SL. Dr. Sam A. Kiger, SMD, provided technical guidance and supervision. Initial investigations were conducted by Mr. Thomas R. Slawson and Ms. Frances M. Warren, SMD.

This report was prepared by Dr. Robert L. Hall, SMD, and edited by Ms. Lee T. Byrne, Information Products Division, Information Technology Laboratory, WES.

COL Dwayne G. Lee, CE, is the Commander and Director of WES. Dr. Robert W. Whalin is Technical Director.

Contents

Conversion Factors, Non-SI to SI (Metric)

Units of Measurement

Non-SI units of measurement used in this report can be converted to SI (metric) units as follows:

Multiply	By	To Obtain
feet	0.3048	metres
inches	25.4	millimetres
kilotons	4.184	terajoules
pounds (force) per square inch	0.006894757	megapascals
pounds (mass)	0.4535924	kilograms
pounds (mass) per cubic foot	16.01846	kilograms per cubic metre
pounds (mass) per foot	1.488164	kilograms per metre
square feet	0.09290304	square metres
tons (mass) per cubic foot	32,036.978	kilograms per cubic metre
tons (mass) per square foot	9,764.856	kilograms per square metre

IMPORTANCE OF RIGID-BODY MOTIONS ON A SINGLE-DEGREE-OF-FREEDOM MODEL

Purpose and Scope

1. The purpose of this study is to determine the effect of rigid-body motion on the single-degree-of-freedom (SDOF) model presently used for dynamic analysis of buried roof slabs. The effect of rigid-body motion is incorporated by adding a second degree of freedom to the model. The second degree will model the motion of the entire structure, which is controlled by the dynamic pressure applied and the resistance of the soil mass. The results of this model should not be interpreted to be more accurate than those produced by the SDOF model. This model is valid only for studying the effect of rigid-body motion since this model has no experimental data or experience to support its results.

2. The results that will be examined are the relative displacements between the roof and the structure. The absolute roof displacements will become larger as a result of the rigid-body motion. However, the relative displacements between the roof and structure are the only displacements that result in damage to the roof. Variations in soil resistance and loading intensity are examined.

Procedure Using Two-Degrees-of-Freedom Model

3. The two-degrees-of-freedom model to be used for this study are shown in Figure 1.

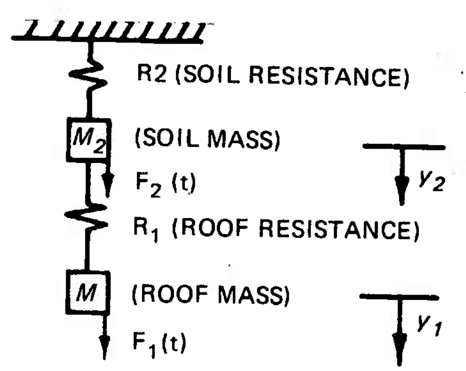

Figure 1. Degree-of-freedom models

4. The roof resistance is a bilinear function based on previous SDOF models. This bilinear function is shown in Figure 2.

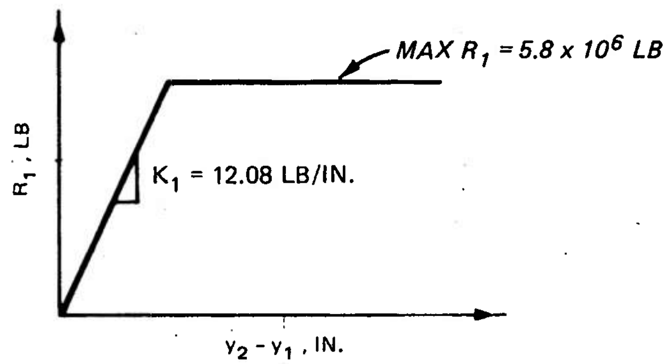

Figure 2. Roof resistance

5. The loading functions F_1 and F_2 are dependent on the pressure-time history of the weapon. The pressure-time (P(t)) relation for the first 50 msec is given in Figure 3. The total pressure duration is taken to be 250 msec, and the pressure is assumed to decay linearly to zero from 50 to 250 msec. Based on the area of roof and foundation, the forcing functions are calculated as follows:

$$F_1(t) = P(t)\ \underset{\text{(dimension of roof)}}{(109.5)(240)}\underset{\text{(soil arching)}}{(0.66)} = 17{,}344.8\ P(t)\ \text{lb}^*$$

$$F_2(t) = P(t)\underset{\text{(assumed foundation dimensions)}}{(145.5)(264)} = 38{,}412\ P(t)\ \text{lb}$$

Soil arching is the ability of a soil to transfer loads from one location to another in response to a relative displacement between the locations.** The total mass of the roof is 855 lb-sec^2/ft. The minimum amount of contributing soil mass from the foundation was assumed to be 5 ft below the foundation. This results in the mass of the foundation being approximately 7,000 lb-sec^2/ft. This mass is based on assuming that the foundation material has a weight of 110 lb/ft^3. The foundation resistance is based on Terzaghi's coefficient of vertical subgrade reaction.† Since a cohesive material is used

* A table of factors for converting non-SI units of measurement to SI (metric) units is presented on page 3.

** S. A. Kiger, T. R. Slawson, and D. W. Hyde. 1984 (Sep). "Vulnerability of Shallow-Buried Flat-Roof Structures; Final Report: A Computational Procedure," Technical Report SL-80-7, Report 6, US Army Engineer Waterways Experiment Station, Vicksburg, Miss.

† Karl Terzaghi. 1985. "Evaluation of Coefficients of Subgrade Reactions," Geotechnique, Vol 5, pp 297-326.

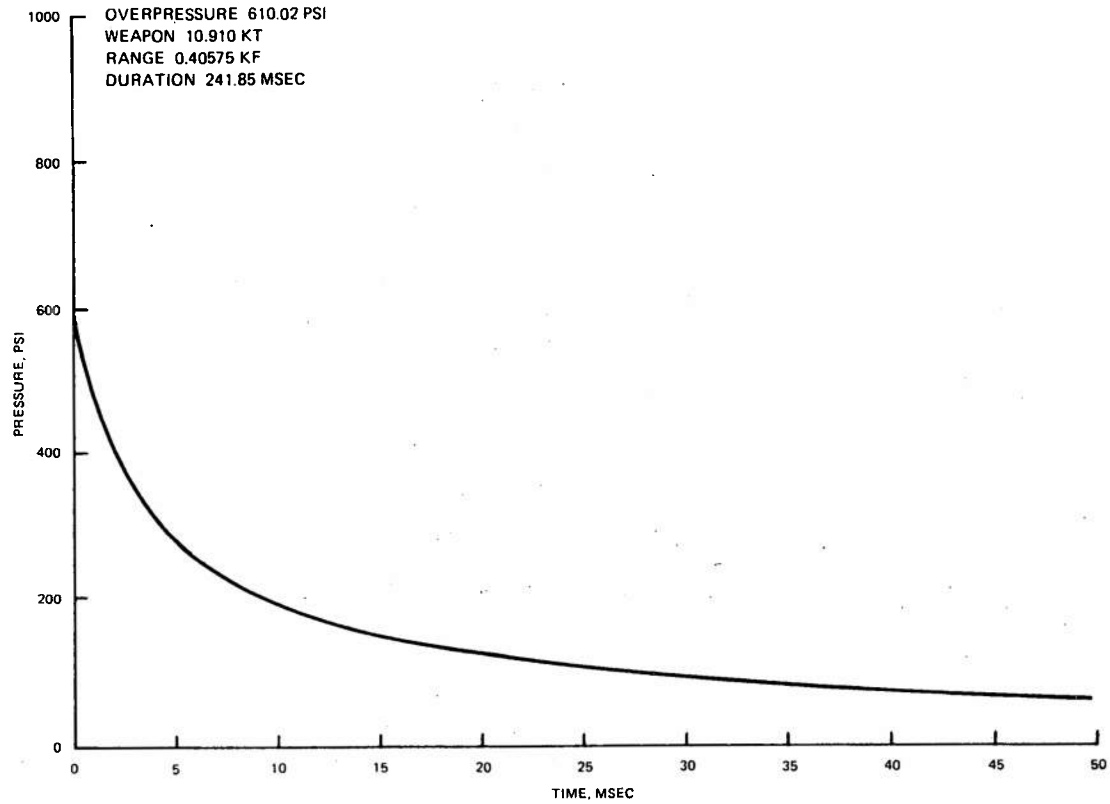

Figure 3. Pressure-time history

around the structure, values for stiff to very stiff clay were used to develop the bilinear resistance curves for the foundation. The calculations for these curves are shown in Appendix A.

6. Two different limiting bilinear curves can be produced using the summary of the data from Appendix A (Figure 4). The K_{min} and K_{max} are based on assuming the foundation material to behave between a stiff to very stiff clay. These are realistic values that will limit the valid ranges of the soil stiffness. However, according to Terzaghi, these values are used for loads not to exceed one-half of ultimate bearing capacity pressure of the

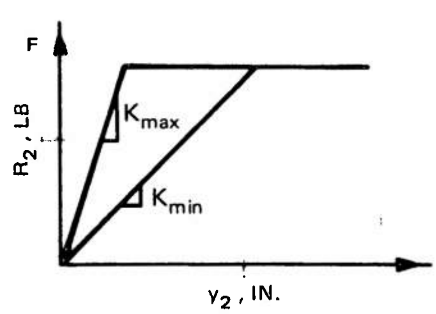

$F = 13 \times 10^6$ LB (FOR MAX SURFACE PRESSURE = 600 PSI)

$K_{max} = 6.7 \times 10^6$ LB/IN.

$K_{min} = 3.4 \times 10^6$ LB/IN.

Figure 4. Soil resistance

structure and also for static loads applied only to structure.* The ultimate bearing capacity is increased with the addition of a surcharge load and thus makes the soil resistance dependent on time. Because the response of the foundation is due to dynamic forces and the force is of short duration, the maximum pressure was assumed for the purpose of calculating the ultimate bearing capacity to always be present at the surface.

7. In addition to changing the properties of the soil resistance, the effect of the rigid-body motion will also be evaluated for additional soil mass and increased dynamic loading. Therefore, load cases 3 and 4 in Table 1 are identical to load cases 1 and 2, except for the increased soil mass. According to Clough and Penzien,** the added mass for a circular section is $1.5\ \rho r^3$, where ρ = weight per unit volume and r = radius. The mass for load cases 3 and 4 is $1.5\ \rho b^3$, where b = the minimum foundation dimension.

8. The relative magnitude of the forcing function is also a major variable controlling the dynamic response of a structure. Therefore, load cases 5 through 8 are identical to load cases 1 through 4, except that the load functions $F_1(t)$ and $F_2(t)$ have been multiplied by a factor of 3 and the maximum force for the soil resistance curve is 36×10^6 lb (see Appendix A).

9. Load cases 9 and 10 have large masses for the foundation and stiff soil resistance curves. These factors will effectively eliminate any rigid-body motion and will produce displacements to compare with other load cases. Load cases 9 should be compared with cases 1 through 4 to determine the effect of rigid-body motion under relatively low pressures and light damage predictions. The results from load case 10 can be used to evaluate load cases 5 through 8, which had relatively high overpressures and heavy damage predictions. Table 1 gives all of the variables for each load case considered.

10. Table 2 summarizes the results of dynamic analysis of the two-degrees-of-freedom models. Plots displaying the displacements of the structure, foundation, and the relative displacements are shown in Appendix B.

11. As seen from Table 2, the rigid-body motion of the foundation and structure can significantly affect the relative displacements between the structure and the roof. When load cases 1 and 2 are compared with load

---

* Karl Terzaghi and Ralph Peck. 1967. Soil Mechanics in Engineering Practice, Wiley, New York.

** Ray W. Clough and Joseph Penzien. 1975. Dynamics of Structures, McGraw-Hill, New York.

Table 1

Model Parameters

Load Case	M_1 lb-sec^2/ in.	M_2 lb-sec^2/ in.	R1M Max Resistance 10^6 lb	K1 10^6 lb/ in.	R2M Max Resistance Soil, 10^6 lb	K_2 10^4 lb/ in.	Maximum Pressure psi
1	71.25	588	5.8	12	13	2.9	610
2	71.25	588	5.8	12	13	5.8	610
3	71.25	1,200	5.8	12	13	2.9	610
4	71.25	1,200	5.8	12	13	5.8	610
5	71.25	588	5.8	12	36	2.9	1,830
6	71.25	588	5.8	12	36	5.8	1,830
7	71.25	1,200	5.8	12	36	2.9	1,830
8	71.25	1,200	5.8	12	36	5.8	1,830
9	71.25	3,000	5.8	12	9,000	9,000	610
10	71.25	3,000	5.8	12	9,000	9,000	1,830

Table 2

Results of Dynamic Analysis of the Two-Degrees-of-Freedom Models

Load Case	$Y_1 - Y_2$ in.	Soil Type	Max Pressure psi
1	1.04	Stiff	610
2	1.01	Very stiff	610
3	1.57	Stiff	610
4	1.59	Very stiff	610
5	118.0	Stiff	1,830
6	114.0	Very stiff	1,830
7	108.0	Stiff	1,830
8	113.0	Very stiff	1,830
9	2.66	Stiff	610
10	109.0	Very stiff	1,830

case 9, the maximum percent difference is 89 percent. When the mass is increased to a more reasonable value (as in load cases 3 and 4), the percent difference with load case 9 becomes 51 percent. However, when the loads are increased, the percent difference decreases, as seen when load cases 5 and 6

are compared with load case 10. This comparison results in a 7.9 percent difference between load cases 7 and 10. When the mass is increased, the percent difference becomes 1 percent between load cases 7 and 10. The two principal factors controlling the relative displacement are the forcing function and the assumed amount of foundation that acts with the structure.

Conclusions

12. These results indicate that at overpressures required to cause severe damage to a relatively hard shallow-buried structure, rigid-body motion will have little effect on the damage predicted from an SDOF analysis. However, at relatively low overpressures, rigid-body motion can result in significantly less damage than would be predicted by an SDOF analysis. Since typical design calculations are for relatively low overpressures (i.e., light damage), it is important to include the effects of rigid-body motion. However, for vulnerability, calculations that predict pressure required to fail the structure, including the effects of rigid-body motion, may not be necessary.

Appendix A

Calculations for Bilinear Soil Resistance Curves

Terzaghi's	Values for Subgrade Modulus*	
Consistency of clay	Stiff	Very stiff
E_S	75 tons/ft^3	150 tons/ft^3

Values valid for pressures $\leq$ one-half of the ultimate bearing capacity q_d where:

$$q_d = 1.2\ cN_c + (\gamma D_f + q)\ N_q + 0.4\ \gamma\ BN_\gamma{}^{**}$$

γ = Unit weight of soil = 115 lb/ft^3

D_f = Height of overburden = 10 ft

B = Width of foundation = 12 ft

C = Cohesion = 1/2 q_u

q = Surcharge load = 600 psi

q_u = Unconfined compressive strength

Consistency of clay	Stiff	Very stiff
q_u (tons/ft^2)	1-2	2-4**
C (tons/ft^2)	0.75	1.5

For 0 = 0

$$N_c = (2 + \pi)$$
$$N_q = 1$$
$$N_\gamma = 0$$

$$qd_{min} = 1.2\ (0.75)\ (5.14)\ (2{,}000)/144 + \left[\frac{(115)\ (10)}{144}\ (600)\right] 1$$

$$qd_{min} = 64.27 + 607.99$$

$$qd_{min} = 672.26 \text{ psi}$$

$$qd_{max} = 1.2\ (1.5)\ (5.14)\ (2{,}000)/144 + \left[\frac{(115)\ (10)}{144}\ (600)\right] 1$$

$$= 128.5 + 607.99$$

$$qd_{max} = 736.49 \text{ psi}$$

$$qd_{min} \simeq qd_{max} = 700 \text{ psi}$$

Note: Bearing capacity is controlled by the loading on ground surface.

$$\frac{\text{Maximum allowable force}}{[P(t)_{max} = 600 \text{ psi}]} = \frac{qDA}{2} = \frac{700\ (145.5)(264)}{2} = 13 \times 10^6 \text{ lb}$$

---

* Karl Terzaghi and Ralph Peck. 1967. Soil Mechanics in Engineering Practice, Wiley, New York.

** Ray W. Clough and Joseph Penzien. 1975. Dynamics of Structures, McGraw-Hill, New York.

$$\frac{\text{Maximum allowable force}}{\left[P(t)_{max} = 1{,}800 \text{ psi}\right]} = \frac{(1{,}900)(145.5)(264)}{2} = 36 \times 10^6 \text{ lb}$$

Spring stiffness, K lb/in.

$$K = \frac{E_s \text{ (connection for rectangular footings) area}}{\text{(connection for larger than } 1 \times 1)}$$

$$K = \frac{E_s(m + 0.5)\ A}{B\ 1.5\ m}$$

M = ratio of rectangular footing sides

$$K_{max} = \frac{E_{s(max)}(m + 0.5)\ A}{B\ 1.5\ m} = \frac{(150)(2{,}000)(0.5511 + 0.5)}{(1{,}728)(1{,}455)1.5(0.5511)}\ (145.5)(264)$$

$$= 5.8 \times 10^4 \text{ lb/in.}$$

$$K_{min} = \frac{E_{s(min)}(m + 0.5)\ A}{B\ 1.5\ m} = \frac{(75)(2{,}000)(0.5511 + 0.5)(145.5)(264)}{(1{,}728)(145.5)(1.5)(0.5511)}$$

$$= 2.9 \times 10^4 \text{ lb/in.}$$

Appendix B

Results of Two-Degrees-of-Freedom Models

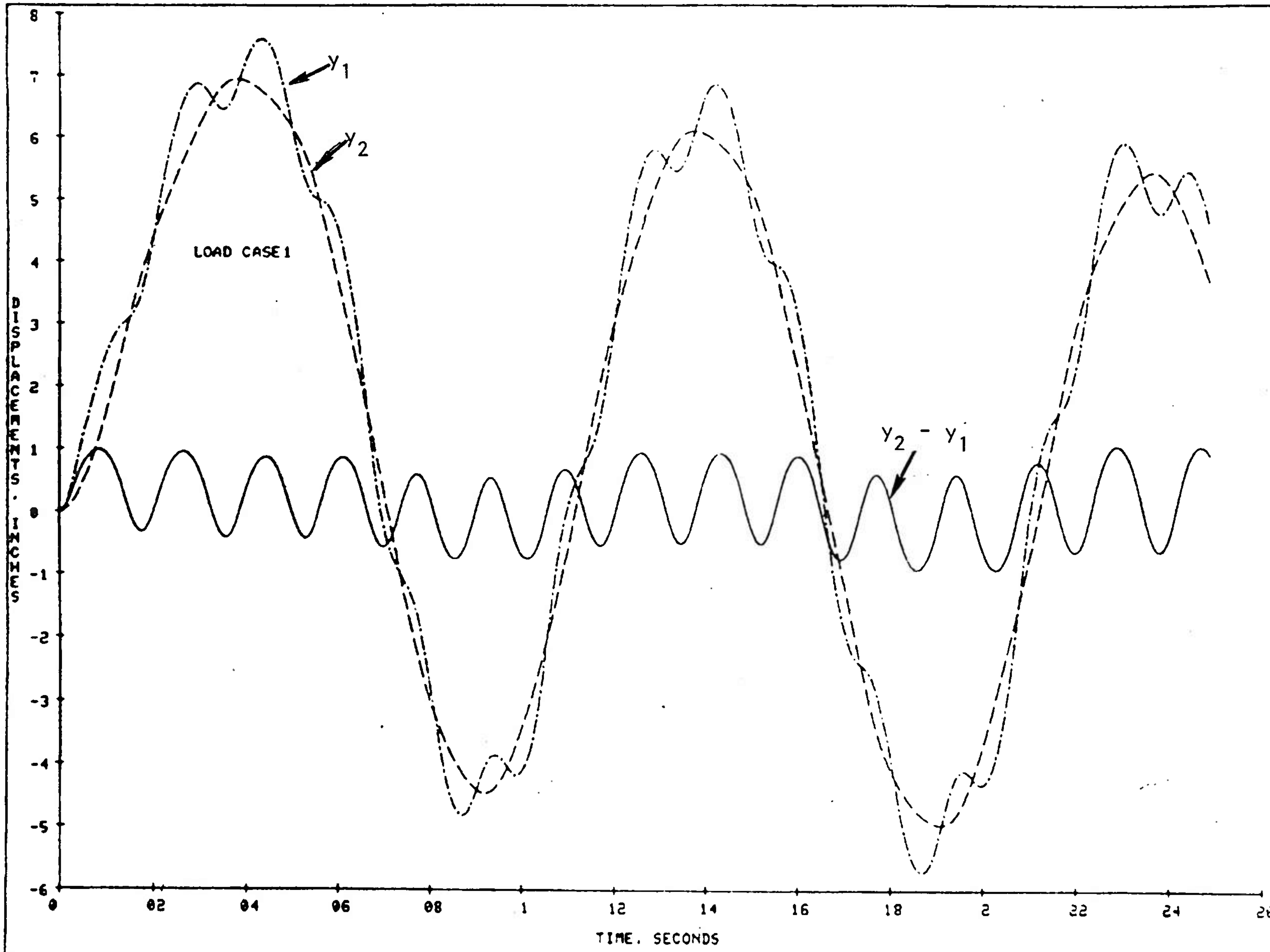

Figure B1. Displacements form two-degrees-of-freedom model for case 1

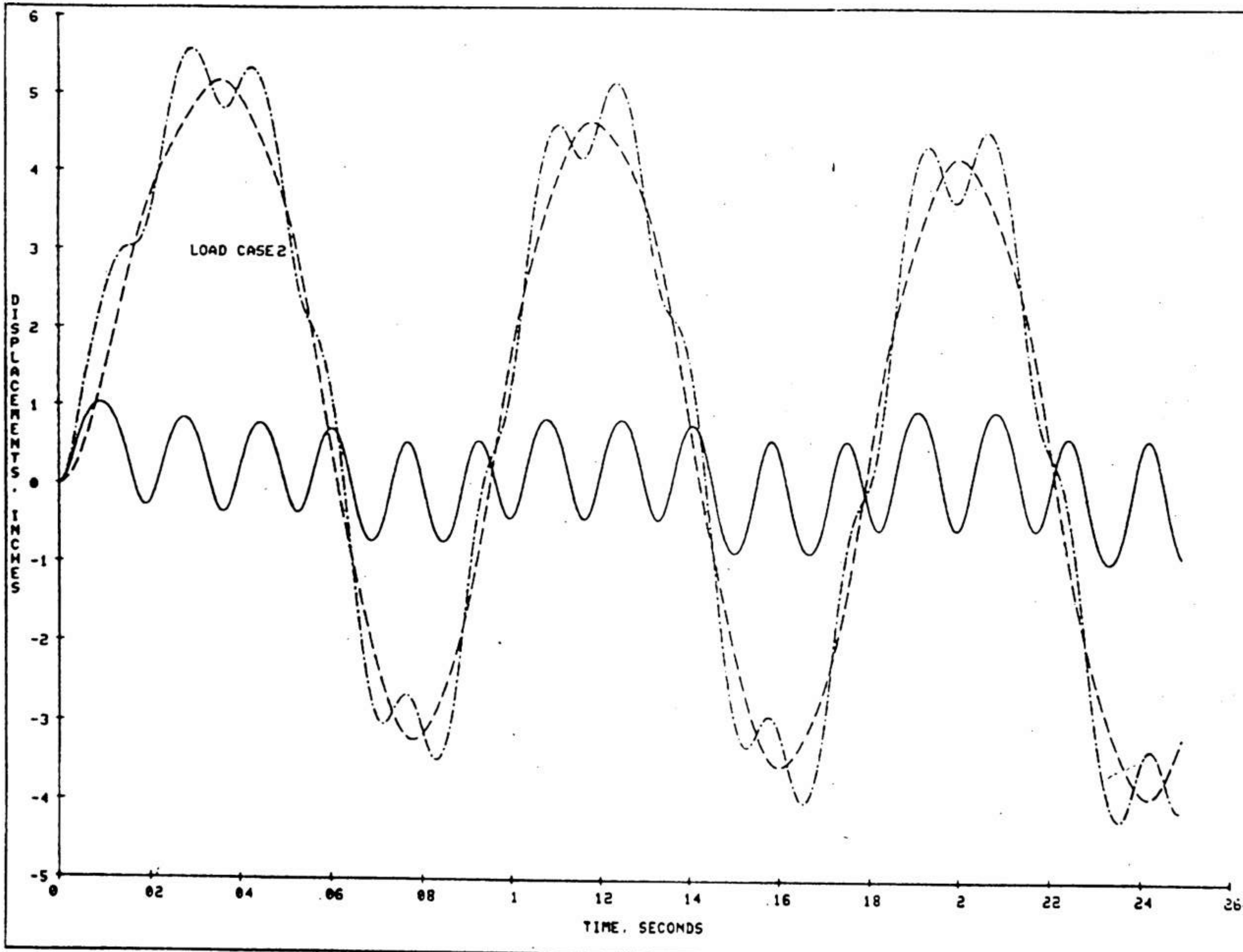

Figure B2. Displacements form two-degrees-of-freedom model for case 2

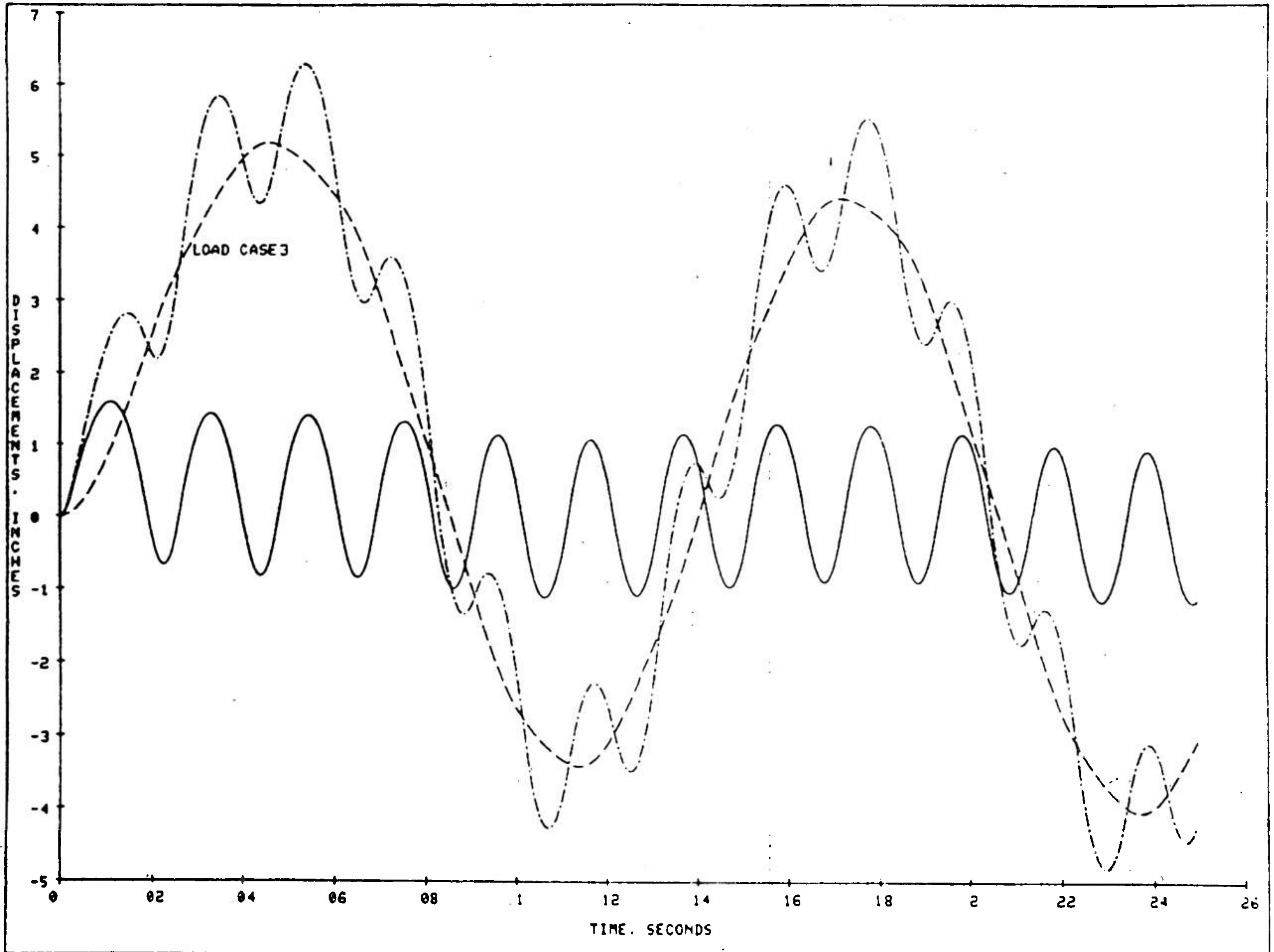

Figure B3. Displacements form two-degrees-of-freedom model for case 3

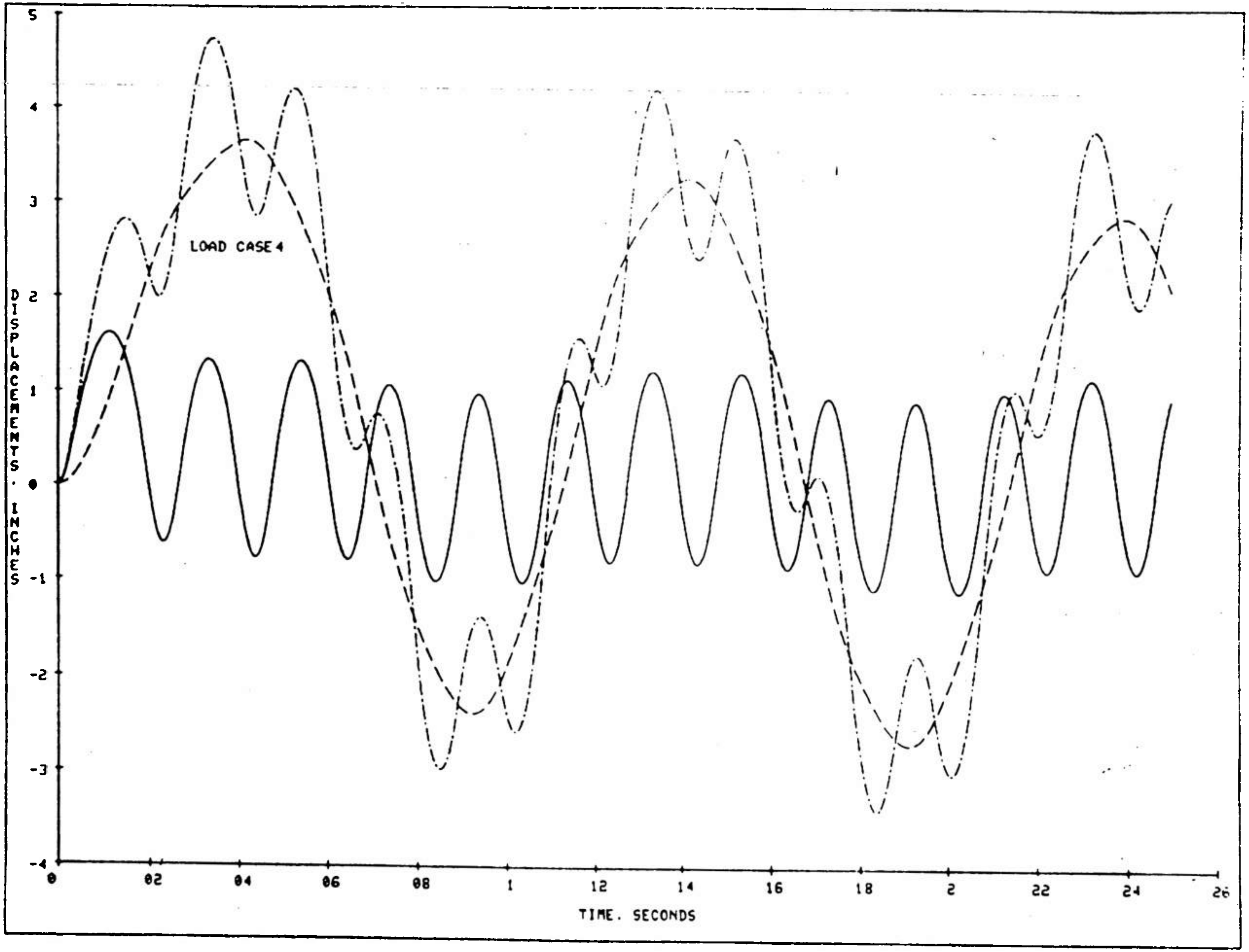

Figure B4. Displacements form two-degrees-of-freedom model for case 4

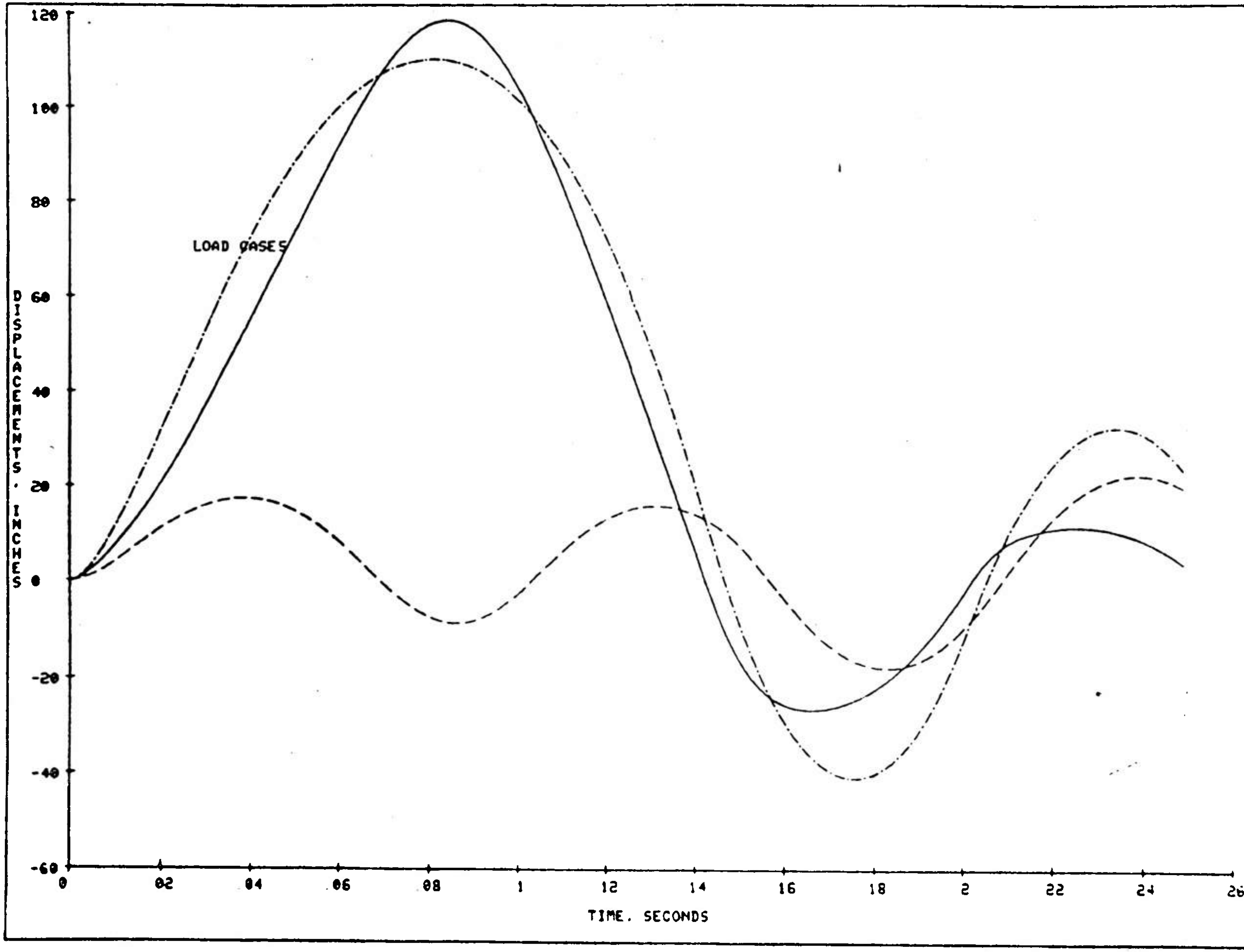

Figure B5. Displacements form two-degrees-of-freedom model for case 5

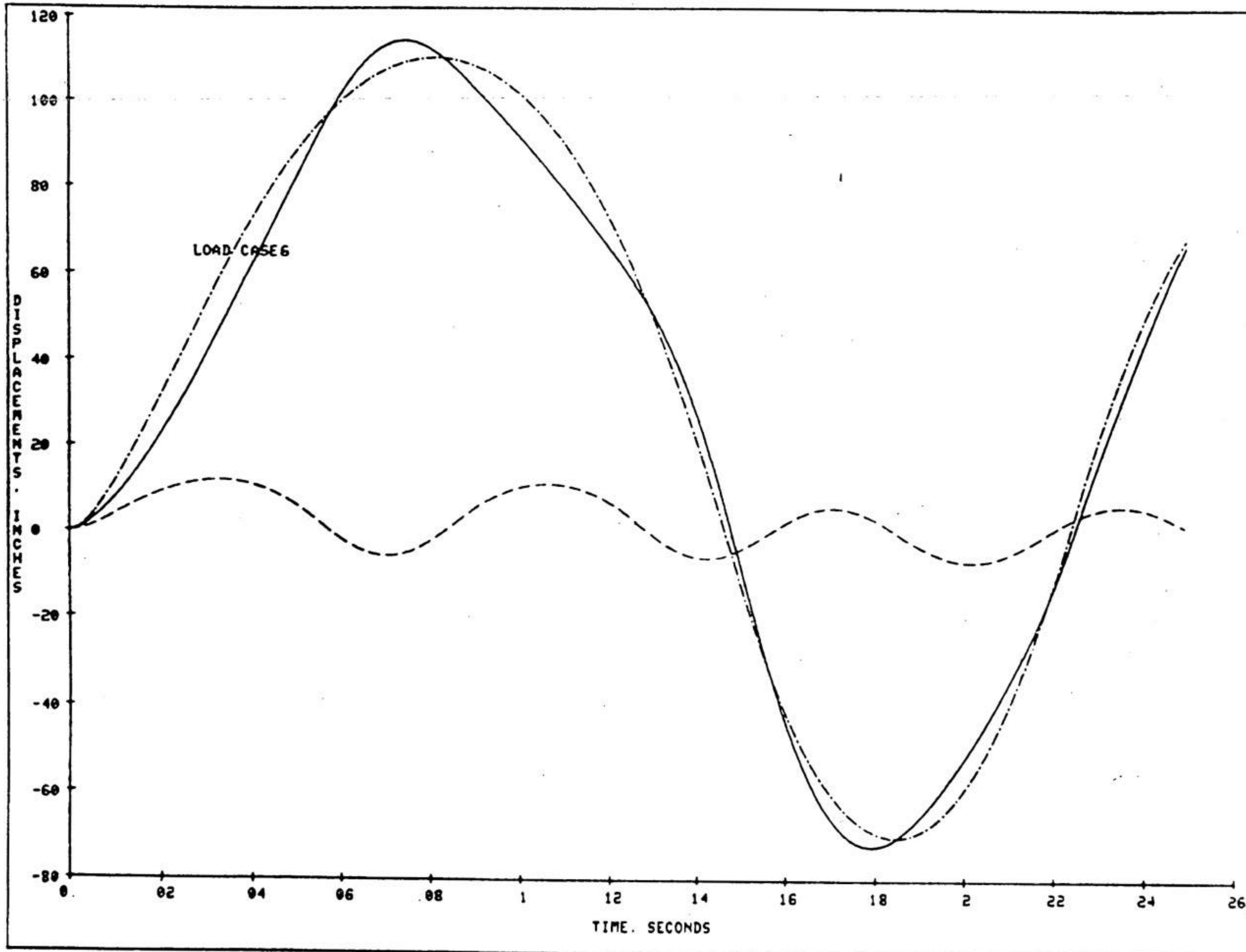

Figure B6. Displacements form two-degrees-of-freedom model for case 6

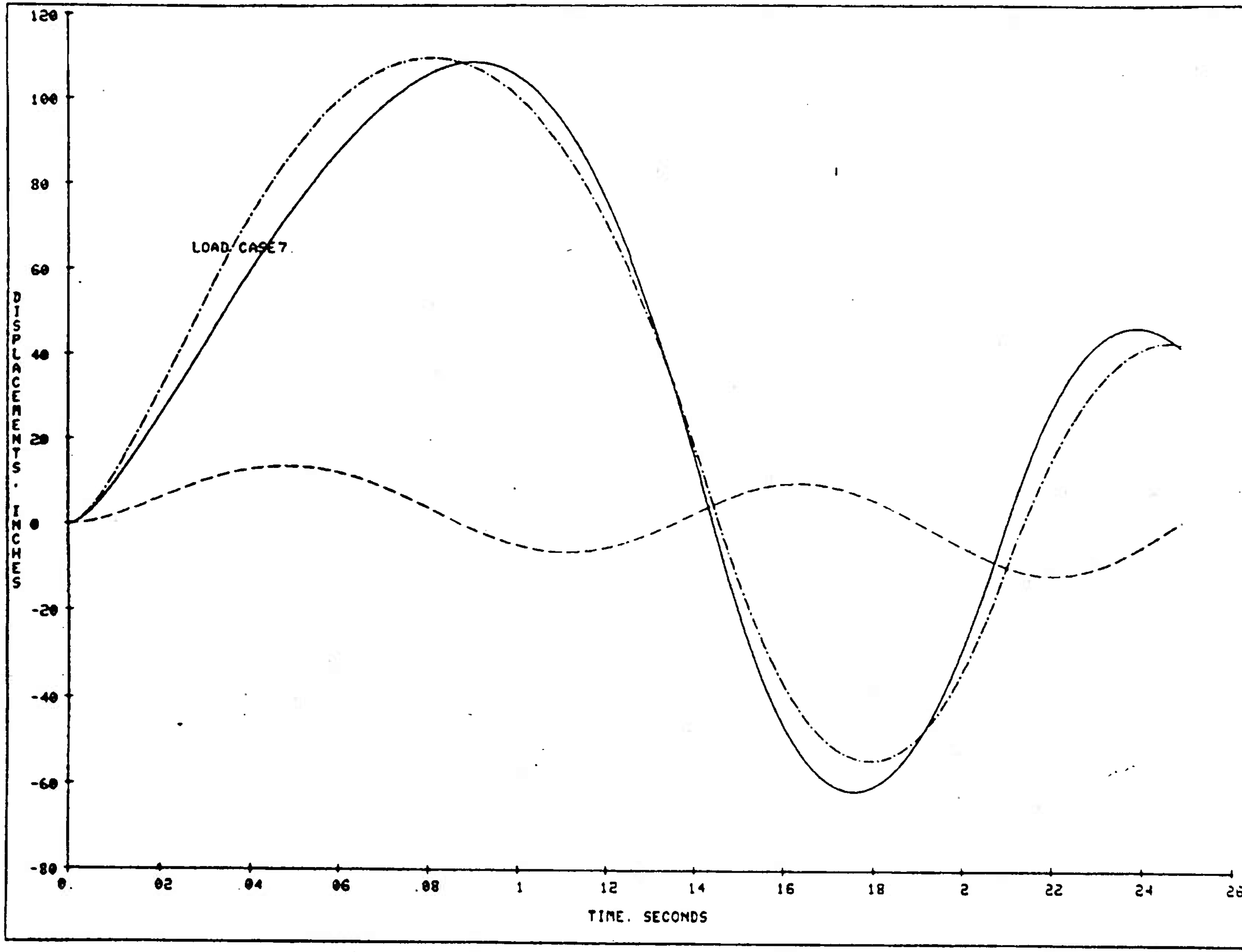

Figure B7. Displacements form two-degrees-of-freedom model for case 7

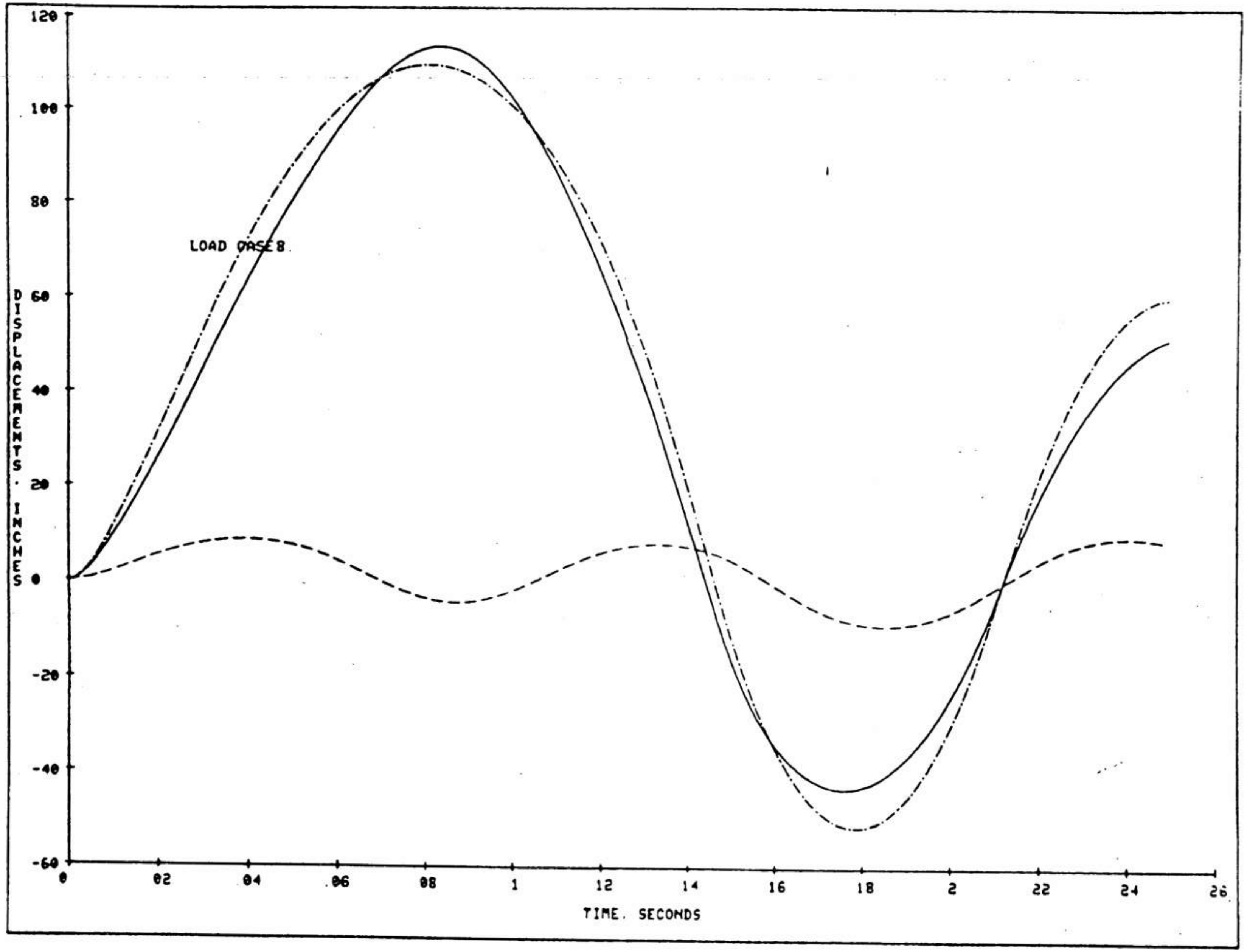

Figure B8. Displacements form two-degrees-of-freedom model for case 8

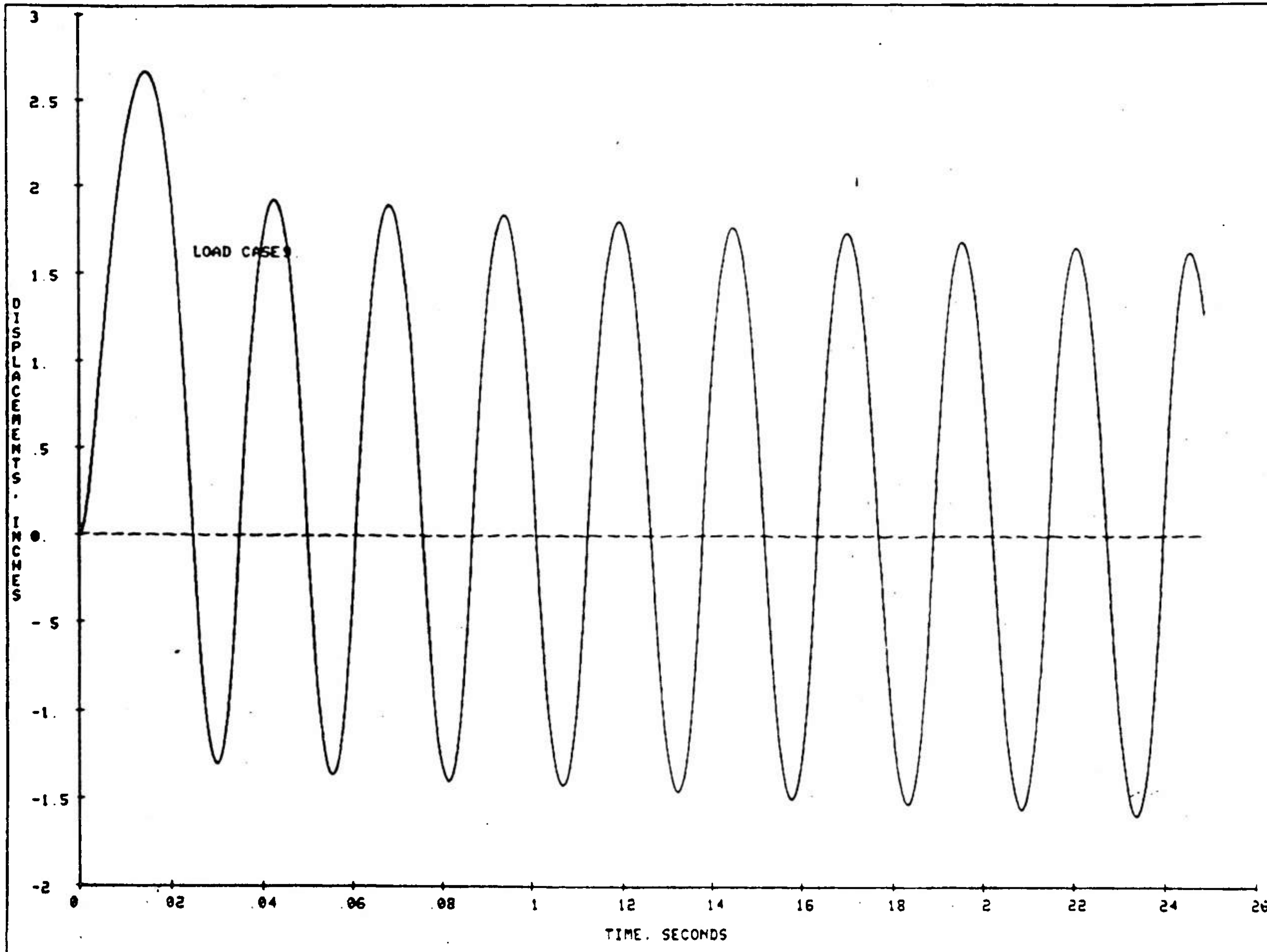

Figure B9. Displacements form two-degrees-of-freedom model for case 9

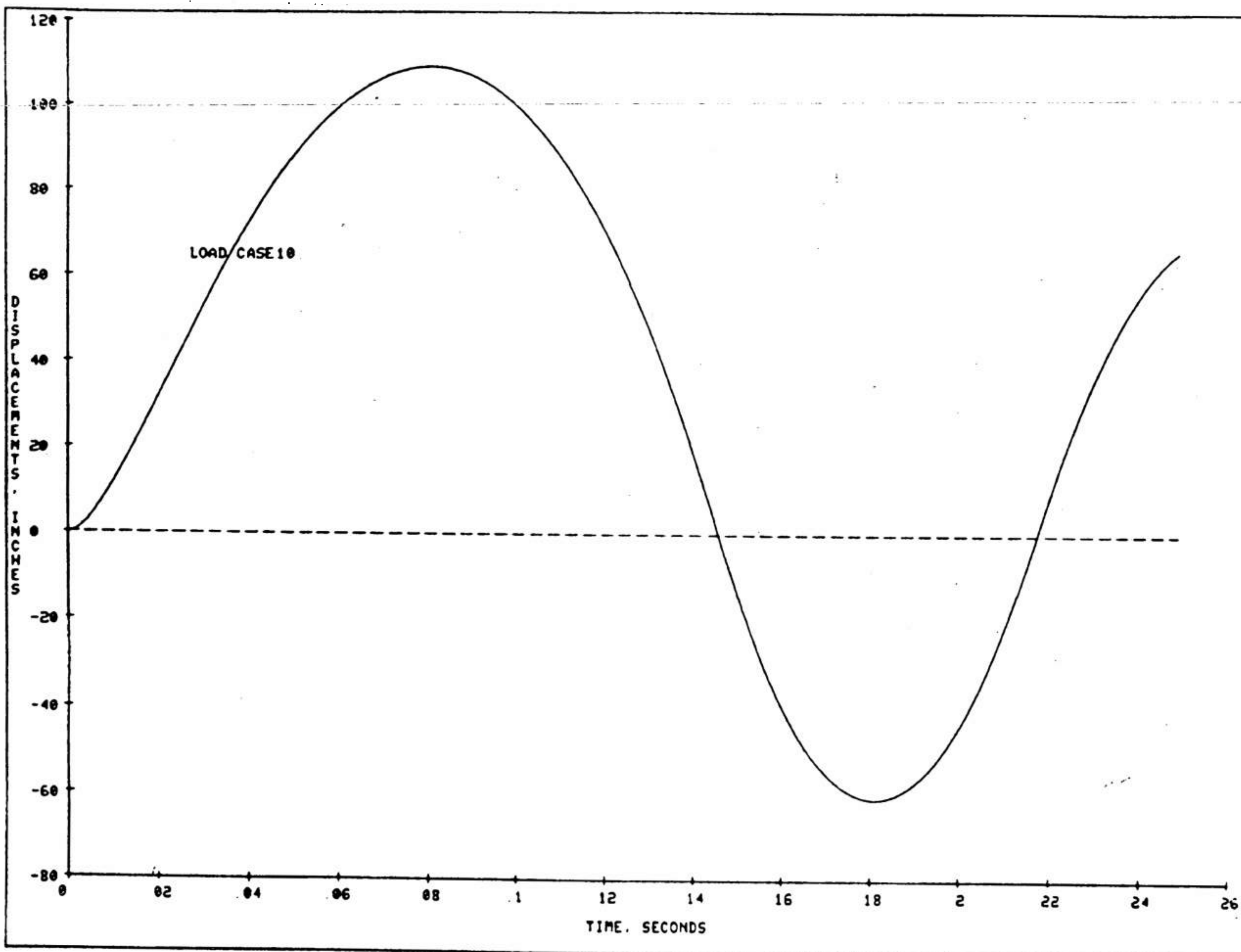

Figure B10. Displacements form two-degrees-of-freedom model for case 10